

# Anion height as a controlling parameter for the superconductivity in iron pnictides and cuprates

Kazuhiko Kuroki<sup>a,b,\*</sup>

<sup>a</sup>Department of Applied Physics and Chemistry, The University of Electro-Communications, Chofu, Tokyo 182-8585, Japan

<sup>b</sup>JST, TRIP, Chofu, Tokyo 182-8585, Japan

## Abstract

Both families of high  $T_c$  superconductors, iron pnictides and cuprates, exhibit material dependence of superconductivity. Here, we study its origin within the spin fluctuation pairing theory based on multi-orbital models that take into account realistic band structures. For pnictides, we show that the presence and absence of Fermi surface pockets is sensitive to the pnictogen height measured from the iron plane due to the multi-orbital nature of the system, which is reflected to the nodeless/nodal form of the superconducting gap and  $T_c$ . Surprisingly, even for the cuprates, which is conventionally modeled by a single orbital model, the multi-orbital band structure is shown to play a crucial role in the material dependence of superconductivity. In fact, by adopting a two orbital model that considers the  $d_{z^2}$  orbital on top of the  $d_{x^2-y^2}$  orbital, we can resolve a long standing puzzle of why the single layered Hg cuprate have much higher  $T_c$  than the La cuprate. Interestingly, here again the apical oxygen height measured from the  $\text{CuO}_2$  plane plays an important role in determining the relative energy difference between  $d_{x^2-y^2}$  and  $d_{z^2}$  orbitals, thereby strongly affecting the superconductivity.

**Keywords:**

Superconductivity, Band structure, Lattice structure, Iron pnictides, Cuprates

**PACS:** ,

## 1. Introduction

Superconductivity in the iron-based pnictide  $\text{LaFeAsO}$  doped with fluorine discovered by Hosono's group[1, 2] and subsequent increase of the transition temperature ( $T_c$ ) in the same family of compounds are remarkable as the first non-copper compound that has  $T_c$ 's exceeding 50 K.[3] Theoretical studies have shown that the electron-phonon coupling is too weak to account for the high  $T_c$ [4], and exploring electronic pairing mechanisms has become a challenge.

An interesting observation of this series of material is their strong material dependence of superconductivity.  $T_c$  ranges from 5K in  $\text{LaFePO}$ [5] to 55K[3] in  $\text{SmFeAsO}$ , where the importance of the lattice structure has been pointed out[6]. A number of experiments on arsenides suggest fully-open superconducting gap, consistent with the proposal of sign reversing  $s$ -wave pairing, [7, 8] but experiments have shown presence of nodes in the superconducting gap of  $\text{LaFePO}$ [9, 10, 11], suggesting that even the gap is material dependent.

The strong material dependence of superconductivity in the pnictides reminds us of the high  $T_c$  cuprates,

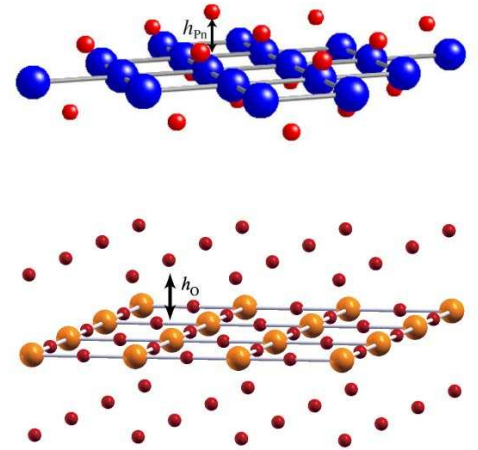


Fig.1 Anion height measured from the cation plane in the iron pnictides (top) and the cuprates (bottom).

which also exhibit strong material dependence of  $T_c$ . It is well known that  $T_c$  varies with the number of layers per unit cell, but an even more basic issue is the significant difference in  $T_c$  within the *single-layered* materials, i.e.,  $\text{La}_{2-x}(\text{Sr/Ba})_x\text{CuO}_4$  with a maximum  $T_c$  of about 40K versus  $\text{HgBa}_2\text{CuO}_{4+\delta}$  with a  $T_c \simeq 90\text{K}$ . Phenomenologically, it has been recognized that the mate-

\*Corresponding author.

Email address: kuroki@vivace.e-one.uec.ac.jp (Kazuhiko Kuroki)

materials with  $T_c \sim 100\text{K}$  tend to have “round” Fermi surfaces, while the Fermi surface of the “low  $T_c$ ” La system is closer to a square shape which implies a relatively better nesting[12, 13].

Conventionally, the cuprates with a rounded Fermi surface have been modeled by a *single-band* model with large second ( $t_2(>0)$ ) and third ( $t_3(<0)$ ) neighbor hopping integrals ( $(|t_2| + |t_3|)/|t_1| \sim 0.4$ ), while the La system has been considered to have smaller  $t_2, t_3$  ( $(|t_2| + |t_3|)/|t_1| \sim 0.1$ ). This, however, has brought about a contradiction between theories and experiments. Namely, while some phenomenological[14] and  $t$ - $J$  model[15, 16] studies give a tendency consistent with the experiments, a number of many-body approaches for the *Hubbard-type* models with realistic values of on-site  $U$  show suppression of superconductivity for large  $t_2 > 0$  and/or  $t_3 < 0$ [17, 18, 19].

In this paper, we show that the experimentally observed material/lattice structure dependence of superconductivity in both pnictides[20] and cuprates[21] can be understood by analyzing the superconductivity within the spin fluctuation pairing theory that takes into account the realistic band structure. A surprising finding is that not only the pnictides, but also the cuprates have band structures where *multiple*  $d$  orbitals play an important role. Interestingly, in both families, the anion height measured from the cation plane (Fig.1) turns out to be one of the key parameters that controls the multiorbital band structure and thus the superconductivity. These studies show that a combination of effective model construction based on first principles band calculation and the application of many body theory can give a realistic description on the material dependence of superconductivity in correlated systems.

## 2. Construction of multiorbital models

### 2.1. Pnictides

We start with the band structure of LaFeAsO. LaFeAsO has a layered structure, where Fe atoms form a square lattice in each layer, which is sandwiched by As atoms. Due to the tetrahedral coordination of As atoms, there are two Fe atoms per unit cell. The experimentally determined lattice constants are  $a = 4.03\text{\AA}$  and  $c = 8.74\text{\AA}$ , with two internal coordinates  $z_{\text{La}} = 0.142$  and  $z_{\text{As}} = 0.651$ . [22] We have first obtained the band structure with plane-wave basis[24], which is then used to construct the maximally localized Wannier functions[23]. These Wannier functions have five orbital symmetries ( $d_{3Z^2-R^2}$ ,  $d_{XZ}$ ,  $d_{YZ}$ ,  $d_{X^2-Y^2}$ ,  $d_{XY}$ , where  $X, Y, Z$  refer to those for this unit cell with two Fe sites as shown in Fig.2(a). The two Wannier orbitals in each unit cell are equivalent in that each Fe atom has the same local arrangement of other atoms. We can then take a unit cell that contains only one orbital per symmetry by unfolding the Brillouin zone, and we end up with an effective five-band model on a square lattice, where  $x$  and  $y$  axes are rotated by 45 degrees from  $X$ - $Y$ . We refer

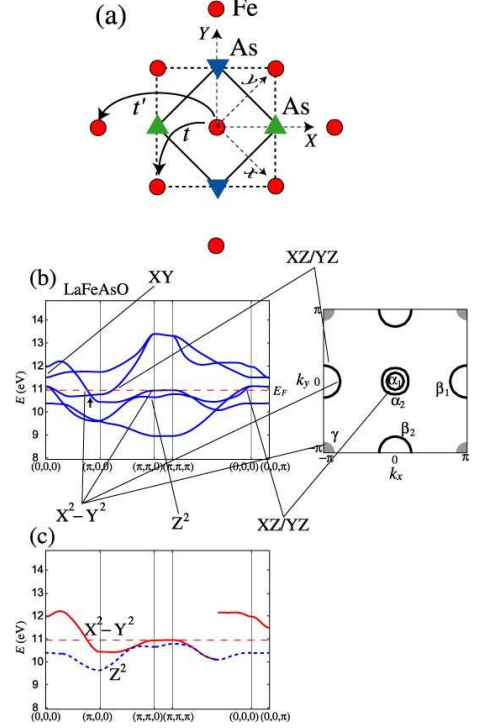


Fig.2 (a) The original (dashed lines) and reduced (solid) unit cells with  $\bullet$  (Fe),  $\nabla$  (As below the Fe plane) and  $\triangle$  (above Fe). (b) The band structure (left) of the five-band model for LaFeAsO, and the Fermi surface (right) at  $k_z = 0$  for  $n = 6.1$ . The main orbital characters of some portions of the bands and the Fermi surface are indicated. The dashed horizontal line in the band structure indicates the Fermi level for  $n = 6.1$ . The short arrow in the band structure indicates the position of the Dirac cone closest to the Fermi level. The gray areas in the Fermi surface around the zone corners represent the  $\gamma$  Fermi surface. (c) The portion of the band that has mainly the  $d_{X^2-Y^2}$  (solid red) and  $d_{Z^2}$  (dashed blue) orbital character.

all the wave vectors in the unfolded Brillouin zone hereafter. We define the band filling  $n$  as the number of electrons/number of sites (e.g.,  $n = 10$  for full filling). The doping level  $x$  in  $\text{LaFeAsO}_{1-x}\text{F}_x$  is related to the band filling as  $n = 6 + x$ .

The five bands are heavily entangled as shown in Fig.2(b) (left) reflecting strong hybridization of the five  $3d$  orbitals, which suggests that the minimal model for the pnictides should include all the five orbitals. In Fig.2(b) (right), the Fermi surface for  $n = 6.1$  (corresponding to  $x = 0.1$ ) obtained by ignoring the inter-layer hoppings is shown in the two-dimensional unfolded Brillouin zone. The Fermi surface consists of four pieces: two concentric hole pockets (denoted here as  $\alpha_1, \alpha_2$ ) centered around  $(k_x, k_y) = (0, 0)$ , two electron pockets around  $(\pi, 0)$  ( $\beta_1$ ) or  $(0, \pi)$  ( $\beta_2$ ), respectively.  $\alpha_i$  ( $\beta_i$ ) corresponds to the Fermi

surface around the  $\Gamma Z$  line (MA in the original Brillouin zone) in the first-principles band calculation.[25] Besides these pieces of the Fermi surface, there is a portion of the band near  $(\pi, \pi)$  that touches the  $E_F$ , so that the portion acts as a “quasi Fermi surface ( $\gamma$ )” around  $(\pi, \pi)$ , which has in fact an important contribution to the spin susceptibility as we shall see below. As for the orbital character,  $\alpha$  and portions of  $\beta$  near Brillouin zone edge have mainly  $d_{XZ}$  and  $d_{YZ}$  character, while the portions of  $\beta$  away from the Brillouin zone edge and  $\gamma$  have mainly  $d_{X^2-Y^2}$  orbital character (see also Fig.2(c)).

To be more precise, the above band structure is sensitive to the lattice structure. In the upper two panels of Fig.3, we compare the band structure of LaFePO and NdFeAsO. A large difference between the two materials lies in the band structure near the wave vector  $(\pi, \pi)$ . In LaFePO, the  $\gamma$  Fermi surface originating from the  $d_{X^2-Y^2}$  band around  $(\pi, \pi)$  largely sinks below the Fermi level, and in turn the  $d_{Z^2}$  band, which is not effective for superconductivity, rises up. On the other hand, in NdFeAsO, the  $d_{X^2-Y^2}$  band rises up even more than in LaFeAsO. The origin of this band structure variation is mainly due to the variation of the pnictogen height  $h_{Pn}$  [20, 25, 26, 27], which varies from  $h_{Pn} = 1.14\text{\AA}$  in LaFePO to  $h_{Pn} = 1.38\text{\AA}$  in NdFeAsO.[6] In fact, in the lower two panels of Fig.3, we show band structures of LaFeAsO with hypothetical lattice structures, where we fix the lattice constants and change only the height to those of NdFeAsO or LaFePO. We can see that the band structure around  $(\pi, \pi)$ , namely, the position of the  $d_{X^2-Y^2}$  and  $d_{Z^2}$  bands are determined by the pnictogen height.

The origin of this height sensitivity of the band structure is the following. In Fig.2(c), we plot the  $d_{X^2-Y^2}$  and  $d_{Z^2}$  portions of the bands. Around  $(\pi, \pi)$ , the lower portion of  $d_{X^2-Y^2}$  and the upper portion of  $d_{Z^2}$  lies close to the  $E_F$ . When the pnictogen height becomes low, the Wannier orbitals widely spread toward the pnictogen, so that the band width tends to become large. Therefore, the  $d_{X^2-Y^2}$  portion around  $(\pi, \pi)$  sinks below  $E_F$ , while the  $d_{Z^2}$  portion rises up.

## 2.2. Cuprates

In contrast to the pnictides, theoretical studies on cuprates has mostly been done for single band models, or the three band model that takes into account the oxygen orbitals that strongly hybridizes with the Cu  $d_{x^2-y^2}$  orbital. As mentioned in the introduction, within these single orbital approaches, it is difficult to understand the experimental observation that the more Fermi surface is rounded, higher the  $T_c$ . To resolve the discrepancy between experimental observations and theory, we consider a *two-orbital* model, where we take into account the  $d_{z^2}$  orbital on top of the  $d_{x^2-y^2}$ [21]. In fact, for the La system, it has long been known that a band with a strong  $d_{z^2}$  character lies rather close to the Fermi energy[28, 29, 30]. More recently, it has been discussed in refs.[31, 12] that

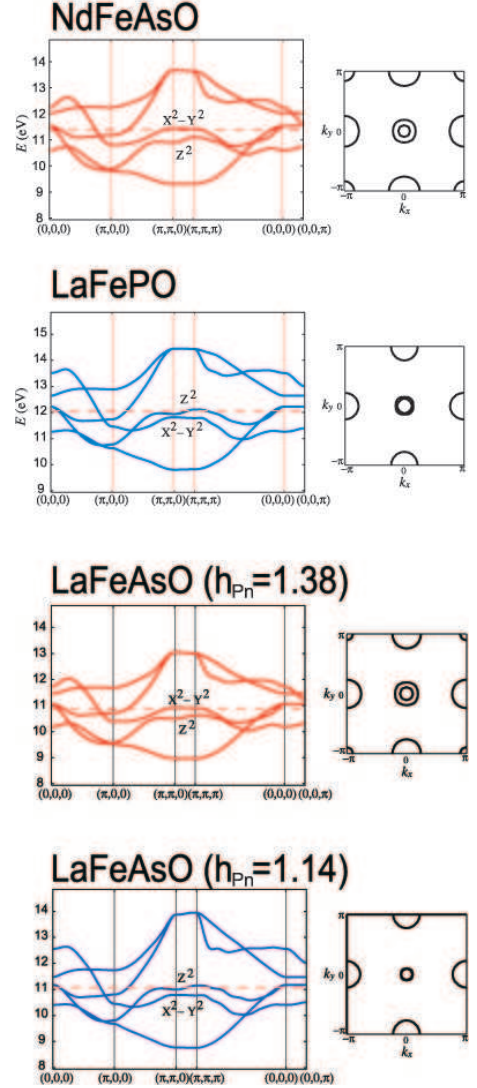


Fig.3 From top to bottom :The band structure and the Fermi surfaces of NdFeAsO, LaFePO, hypothetical structure of LaFeAsO with  $h_{Pn} = 1.38\text{\AA}$  and  $1.14\text{\AA}$ .

the shape of the Fermi surface is determined by the energy level of the “axial state” consisting of a mixture of Cu  $d_{z^2}$ -O  $p_z$  and Cu  $4s$  orbitals, and that the strength of the  $d_{z^2}$  contribution causes the difference in the Fermi surface shape between the La and Hg systems. Namely, the  $d_{z^2}$  contribution is large in the La system making the Fermi surface closer to a square, while the contribution is small in the Hg system making the Fermi surface more rounded. In Fig.4, we show the first-principles[24] result for band structures in the two-orbital model for the La and Hg systems, obtained by constructing maximally localized Wannier orbitals[23]. The lattice parameters adopted here are experimentally determined ones for the doped materials[32, 33]. We can confirm that in the La system the main band (usually considered as the “ $d_{x^2-y^2}$  band”)

has in fact a strong  $d_{z^2}$  character on the Fermi surface near the N point, which corresponds to the wave vectors  $(\pi, 0), (0, \pi)$  in the Brillouin zone of the square lattice. The  $d_{z^2}$  contribution is seen to “push up” the van Hove singularity (vHS) of the main band, resulting in a seemingly well nested (square shaped) Fermi surface. In the Hg system, on the other hand, the  $d_{z^2}$  band stays well away from  $E_F$ , and consequently the vHS is lowered, resulting in a rounded Fermi surface.

If we estimate in the two-orbital model the ratio  $(|t_2| + |t_3|)/|t_1|$  within the  $d_{x^2-y^2}$  orbitals, we get 0.35 for the La system against 0.41 for Hg, which are rather close to each other. This contrasts with the situation in which the model is constrained into a single band model that considers one kind of Wannier orbital to reproduce the main band that intersects the Fermi energy. There, the Wannier orbital has mainly  $d_{x^2-y^2}$  character, but has “tails” with a  $d_{z^2}$  character especially for the La system. Then the ratio  $(|t_2| + |t_3|)/|t_1|$  in the single-orbital model reduces to 0.14 for La against 0.37 for Hg, which is just the conventional view mentioned in the Introduction. From this, we can confirm that it is the  $d_{z^2}$  contribution that makes the Fermi surface in the La system square shaped, while the “intrinsic” Fermi surface of the high  $T_c$  cuprate family is, as in the Hg system, rounded (which is actually due to the

Cu 4s orbital as shown in Ref.[31, 12], whose contribution is effectively considered in the present model).

### 3. Many-body Hamiltonian

For the many body part of the Hamiltonian, we consider the standard interaction terms that comprise the intra-orbital Coulomb  $U$ , the inter-orbital Coulomb  $U'$ , the Hund’s coupling  $J$  and the pair-hopping  $J'$ . The many body Hamiltonian then reads

$$H = \sum_i \sum_\mu \sum_\sigma \varepsilon_\mu n_{i\mu\sigma} + \sum_{ij} \sum_{\mu\nu} \sum_\sigma t_{ij}^{\mu\nu} c_{i\mu\sigma}^\dagger c_{j\nu\sigma} + \sum_i \left[ U \sum_\mu n_{i\mu\uparrow} n_{i\mu\downarrow} + U' \sum_{\mu>\nu} \sum_{\sigma,\sigma'} n_{i\mu\sigma} n_{i\nu\sigma'} - J \sum_{\mu\neq\nu} \mathbf{S}_{i\mu} \cdot \mathbf{S}_{i\nu} + J' \sum_{\mu\neq\nu} c_{i\mu\uparrow}^\dagger c_{i\mu\downarrow}^\dagger c_{i\nu\downarrow} c_{i\nu\uparrow} \right], \quad (1)$$

where  $i, j$  denote the sites and  $\mu, \nu$  the orbitals, and  $t_{ij}^{\mu\nu}$  is the transfer energy obtained from the maximally localized Wannier orbitals.

For these models, we apply spin fluctuation theory and solve the Eliashberg equation to analyze superconductivity. Multiorbital random phase approximation (RPA) is described in e.g. Refs.[34, 35]. In the present case, Green’s function  $G_{lm}(k)$  ( $k = (\mathbf{k}, i\omega_n)$ ) is a  $m \times m$  matrix, where  $m$  is the number of orbitals. The irreducible susceptibility matrix

$$\chi_{l_1, l_2, l_3, l_4}^0(q) = - \sum_k G_{l_1 l_3}(k+q) G_{l_4 l_2}(k) \quad (2)$$

( $l_i = 1, \dots, m$ ) has  $m^2 \times m^2$  components, and the spin and the charge (orbital) susceptibility matrices are obtained from matrix equations,

$$\chi_s(q) = \frac{\chi^0(q)}{1 - S\chi^0(q)} \quad (3)$$

$$\chi_c(q) = \frac{\chi^0(q)}{1 + C\chi^0(q)} \quad (4)$$

where

$$S_{l_1 l_2, l_3 l_4}, \quad C_{l_1 l_2, l_3 l_4} = \begin{cases} U, & U & l_1 = l_2 = l_3 = l_4 \\ U', & -U' + J & l_1 = l_3 \neq l_2 = l_4 \\ J, & 2U' - J, & l_1 = l_2 \neq l_3 = l_4 \\ J', & J' & l_1 = l_4 \neq l_2 = l_3 \end{cases}$$

The Green’s function and the effective singlet pairing interaction,

$$V^s(q) = \frac{3}{2} S\chi^s(q)S - \frac{1}{2} C\chi^c(q)C + \frac{1}{2}(S + C), \quad (5)$$

are plugged into the linearized Eliashberg equation,

$$\lambda \phi_{l_1 l_4}(k) = -\frac{T}{N} \sum_q \sum_{l_2 l_3 l_5 l_6} V_{l_1 l_2 l_3 l_4}(q) \times G_{l_2 l_5}(k-q) \phi_{l_5 l_6}(k-q) G_{l_3 l_6}(q-k) \quad (6)$$

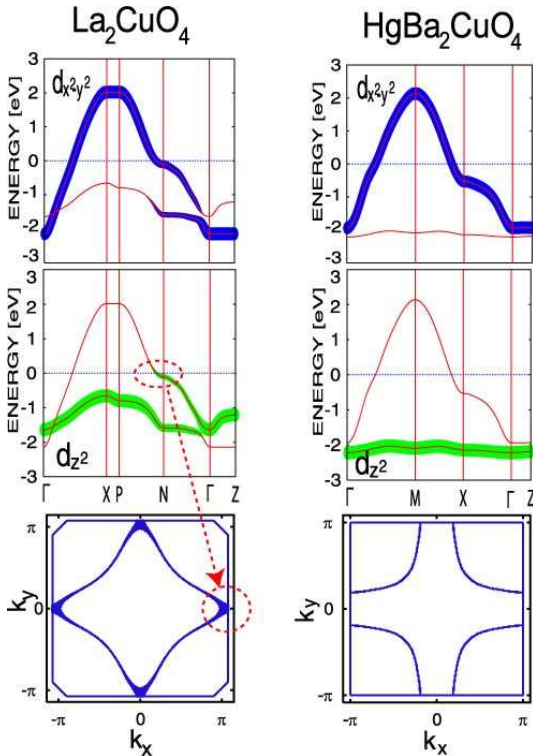


Fig.4 The band structure of the two ( $d_{x^2-y^2}$ - $d_{z^2}$ ) orbital model for  $\text{La}_2\text{CuO}_4$  (left) and  $\text{HgBa}_2\text{CuO}_4$  (right). The top (middle) panels depict the strength of the  $d_{x^2-y^2}$  ( $d_{z^2}$ ) characters with thickened lines, while the bottom panels show the Fermi surfaces (for a total band filling  $n = 2.85$ ).



Here,  $T_c$  is the temperature where the eigenvalue  $\lambda$  reaches unity, so when  $\lambda$  is calculated at a fixed temperature for different situations/materials, the value can be considered as a qualitative measure for the  $T_c$ .

#### 4. Anion height dependence of superconductivity

##### 4.1. Pnictides

We first look into the superconductivity of pnictides. We apply RPA to the 5 orbital model, where we take  $U = 1.2$ ,  $U' = 0.9$ ,  $J = J' = 0.15\text{eV}$ , the temperature is fixed at  $T = 0.02\text{ eV}$  and  $32 \times 32 \times 4$   $k$ -point meshes and 512 Matsubara frequencies are taken. Let us first look at the the spin susceptibility of LaFeAsO. In the top panels of Fig.5, we show  $\chi_{s3333}$  and  $\chi_{s4444}$ , which represent the spin correlation within  $d_{YZ}$  and  $d_{X^2-Y^2}$  orbitals, respectively.  $\chi_{s3333}$  peaks solely around  $(\pi, 0)$  and  $(0, \pi)$ , which reflects the nesting between the  $XZ, YZ$ -charactered portions of  $\alpha$  and  $\beta$  Fermi pockets as shown in a bottom panel of Fig.5. On the other hand,  $\chi_{s4444}$  has peaks around  $(\pi, 0)$ ,  $(0, \pi)$  and around  $(\pi, \pi/2)/(\pi/2, \pi)$  as well. The former is due to the nesting between the  $\gamma$  quasi Fermi surface and the  $d_{X^2-Y^2}$  portion of the  $\beta$  Fermi surface as was first pointed out in ref.[7], while the latter originates from the nesting between the  $d_{X^2-Y^2}$  portion of the  $\beta_1$  and  $\beta_2$  Fermi surfaces.[8] The  $(\pi, 0)$ ,  $(0, \pi)$  feature is consistent with the stripe (i.e., collinear) antiferromagnetic order for the undoped case, which was suggested by transport and optical reflectance[36], and further confirmed by neutron scattering experiments.[22] The stabilization of such an antiferromagnetic ordering has also been pointed out in first principles calculations.[37, 36, 38] Furthermore, the presence of spin fluctuations near the wavevector  $(\pi, 0)$ ,  $(0, \pi)$  in the *unfolded Brillouin zone* has indeed been confirmed in an inelastic neutron scattering experiment[39].

When the pairing is mediated by spin fluctuations, the gap on the Fermi surface tends to change its sign across the wave vector at which the spin fluctuations develop. Since there are multiple spin fluctuation modes in our model, the superconducting gap should be determined by the co-operation or competition between these multiple modes. Specifically, the  $\alpha$ - $\beta$  and  $\gamma$ - $\beta$  nestings tend to favor the fully-gapped, sign-reversing  $s$ -wave ( $s\pm$ -wave), in which the gap changes sign between  $\alpha$  and  $\beta$  and also between  $\gamma$  and  $\beta$ , but has a constant sign on each pocket as shown in Fig.5.[7]. This kind of gap has in fact been considered in the context of raising  $T_c$  in spin fluctuation mediated pairing in that the nodes of the gap, which is a necessary evil for spin fluctuation mediated pairing, do not have to intersect the Fermi surface[40, 41]. On the other hand,  $\beta_1$ - $\beta_2$  nesting tends to change the sign of the gap between these pockets, which can result in either  $d$ -wave or an  $s$ -wave pairing with nodes on the  $\beta$  Fermi surface, as shown in Fig.5 [42, 20].

When the pnictogen atom is at low positions, the  $\beta - \gamma$  nesting is not effective, and the competition between

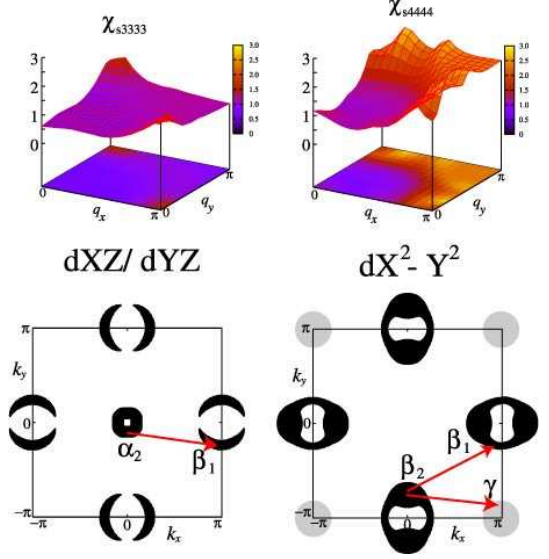


Fig.5 Top panel: RPA result of the diagonal component of the spin susceptibility matrix,  $\chi_{s3333}$ (left) and  $\chi_{s4444}$ (right) (3 :  $YZ$ , 4 :  $X^2 - Y^2$ ) for LaFeAsO. Bottom panel: Nesting is shown for the Fermi surface for orbitals  $XZ, YZ$  (left) and for  $X^2 - Y^2$  (right). Here the thickness of the Fermi surface represents the strength of the respective orbital character. The gray areas around the corners in the left panel indicates the  $\gamma$  “quasi” Fermi surface.

$(\pi/0)/(0, \pi)$  and  $(\pi, \pi/2)/(\pi/2, \pi)$  spin fluctuations results in a frustration in momentum space, where the gap tends to change the sign of the gap across these vectors. Consequently, the  $s$ -wave gap has nodes intersecting the  $\beta$  Fermi surface, and this pairing is nearly degenerate with  $d$ -wave pairing. When the pnictogen is high, the  $\beta$ - $\gamma$  nesting becomes more effective than the  $\beta_1$ - $\beta_2$  nesting, and the two kinds of  $(\pi/0)/(0, \pi)$  spin fluctuations, those originating from  $d_{XZ}/d_{YZ}$  and  $d_{X^2-Y^2}$  orbitals, cooperates without experiencing frustration to result in the fully gapped  $s\pm$ -wave pairing.

The absence/presence of the frustration affects also the strength of the superconducting instability, where the fully gapped case has a stronger tendency toward pairing. This can be seen from the eigenvalue of the Eliashberg equation plotted as a function of the pnictogen height in the bottom panel of Fig.6, where we adopt the 5 band model for LaFeAsO, but vary the height. Thus the pnictogen height  $h_{\text{Pn}}$  acts as a switch between higher  $T_c$  nodeless and low  $T_c$  nodal pairings, which explains the difference between NdFeAsO and LaFePO in both  $T_c$  and the gap.

Here, we have focused on the effect of the  $\gamma$  Fermi surface around  $(\pi, \pi)$  in the context of the lattice structure dependence, but its effect has recently been studied in detail from the viewpoint of the electron-electron interaction and the band filling [43, 44]. Also, a real space picture for the presence/absence of the nodes in the gap has been discussed[45]. The electron correlation effects beyond

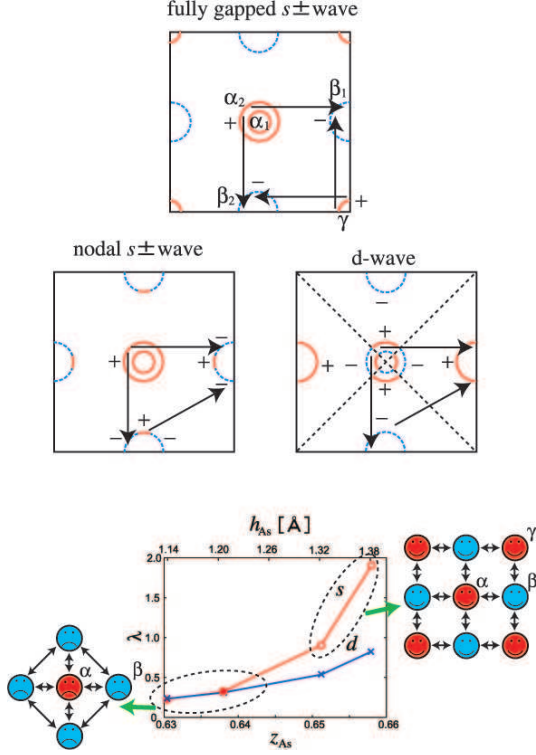


Fig.6 Top and middle panels: the fully-gapped  $s\pm$  wave, the nodal  $s\pm$  wave and  $d$  wave gap are schematically shown. The solid red (dashed blue) curves represent positive (negative) sign of the gap. The arrows indicate the dominating nesting vectors. Bottom: the  $s$ -wave and  $d$ -wave eigenvalues of the Eliashberg equation plotted as functions of As height for the hypothetical lattice structure of LaFeAsO. The figures in the left and right insets show schematically the presence or absence of frustration.

RPA has also been taken into account in the fluctuation exchange (FLEX) study[44, 46] and a functional renormalization group study[47], which also finds a similar effect of the  $\gamma$  Fermi surface on the presence/absence of nodes in the superconducting gap.

The above scenario is consistent with the presence of line nodes in the superconducting gap of the low  $T_c$  phosphides [9, 10, 11]. On the other hand, the fully gapped  $s\pm$ -wave is difficult to detect experimentally because the absolute value of the gap is essentially the same as that of a simple  $s$ -wave gap, with no characteristic angular dependence. Nevertheless, a recent phase sensitive STM experiment has clearly detected the sign reverse between the Fermi surfaces separated by  $(\pi, 0)$ ,  $(0, \pi)$ [48].

#### 4.2. Cuprates

We now move on to the superconductivity in the cuprates. For the electron-electron interactions, we take  $U = 3.0\text{eV}$ ,  $J = J' = 0.3\text{eV}$ , which gives the interorbital  $U' = U - 2J = 2.4\text{eV}$ . The temperature is fixed

at  $k_B T = 0.01\text{eV}$ . As for the band filling (number of electrons/site), we concentrate on the total  $n = 2.85$ , for which the main band has 0.85. Here we apply the multiorbital FLEX[34, 49, 50], which takes into account the self-energy correction to the Green's function self-consistently, for the three-dimensional lattice taking  $32 \times 32 \times 4$   $k$ -point meshes and 1024 Matsubara frequencies.

Here again, we focus on how the anion height, namely, the apical oxygen height measured from the  $\text{CuO}_2$  plane affects the band structure and hence superconductivity. This is motivated by the fact that the energy level offset between  $d_{x^2-y^2}$  and  $d_{z^2}$  orbitals should be controlled (at least partially) by the ligand field, hence by the height,  $h_O$ , of the apical oxygen[29]. To single out this effect, let us examine the two-orbital model of the La cuprate for which we increase  $h_O$  from its original value  $2.41\text{\AA}$  with other lattice parameters fixed. In Fig.7(a), we plot the Eliashberg equation eigenvalue of the  $d$ -wave superconductivity as a function of  $h_O$ . We can see that  $\lambda$  monotonically increases with the height. As seen from the inset of Fig.7(b),  $\Delta E$ , defined as the difference of the on-site energy between  $d_{x^2-y^2}$  and  $d_{z^2}$  orbitals, is positively correlated with  $h_O$  as expected, and importantly, Fig.7(b) shows that the increase in  $\lambda$  is positively correlated with the increase in  $\Delta E$ . Hence the superconductivity turns out to be enhanced as the  $d_{z^2}$  band moves away from the main band. Note that this occurs *despite the Fermi surface becoming more rounded* with larger  $\Delta E$ , namely, the effect of the orbital character (smaller  $d_{z^2}$  contribution) dominates over the Fermi surface shape effect. Conversely, the strong  $d_{z^2}$  orbital character in the Fermi surface around the wave vectors  $(\pi, 0)$ ,  $(0, \pi)$  works destructively against  $d$ -wave superconductivity. Physically, this may be understood as follows.  $d$ -wave superconductivity occurs due to pair scattering from  $\sim (\pi, 0)$  to  $\sim (0, \pi)$  and vice versa mediated by antiferromagnetic spin fluctuations (Fig.7(c)). When the states around  $(\pi, 0)$ ,  $(0, \pi)$  has strong  $d_{z^2}$  character, superconductivity is suppressed since  $d$ -wave pairing has a rough tendency for higher  $T_c$  in bands that are nearly half filled, whereas the  $d_{z^2}$  orbital here is nearly full filled (has holes only around  $(\pi, 0)$ ,  $(0, \pi)$ ).

In Fig.7, we have also plotted the corresponding values of the Hg system obtained with the actual lattice structure. We can see that  $\Delta E$  in Hg is indeed larger than that in La as expected, but actually  $\Delta E \simeq 2.2\text{eV}$  for Hg is larger than  $\Delta E \simeq 1.3\text{eV}$ , which is the value the La system would take for  $h_O = 2.8\text{\AA}$ . Consequently,  $\lambda$  for Hg is somewhat larger than that for the La system with the same value of  $h_O$ . This implies that there are also some effects other than the apical oxygen height that also enhance  $\Delta E$  (i.e., lower the  $d_{z^2}$  level with respect to the  $d_{x^2-y^2}$  level) in the Hg system, thereby further favoring  $d$ -wave superconductivity. In this context, the present result reminds us of the so-called ‘‘Maekawa’s plot’’, where a positive correlation between  $T_c$  and the level of the apical oxygen  $p_z$  hole was pointed out[51]. Since a higher  $p_z$  hole level (i.e., a lower  $p_z$  electron level) is likely to lower

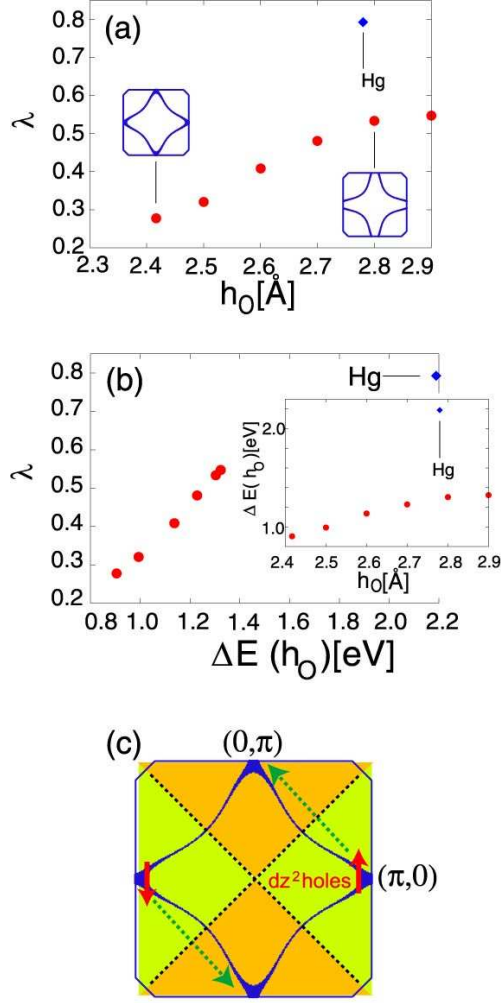


Fig.7 The eigenvalue of the Eliashberg equation  $\lambda$  (red circles) when  $h_O$ (a) or  $\Delta E$ (b) is varied hypothetically in the lattice structure of  $\text{La}_2\text{CuO}_4$ . Blue diamond indicates the eigenvalue of  $\text{HgBa}_2\text{CuO}_4$ . Inset in (b) shows the relation between  $h_O$  and  $\Delta E$ . In (c), the pair scattering of  $d_{z^2}$  holes around  $(\pi, 0)$   $(0, \pi)$  is illustrated.

$E_{z^2}$  because the  $d_{z^2}$  Wannier orbital in our model consists mainly of  $\text{Cu}3d_{z^2}$  and apical oxygen  $2p_z$  orbitals, the positive correlation between  $\Delta E$  and  $T_c$  found here is indeed consistent with Maekawa's plot.

## 5. Conclusion

In this paper, we have focused on the origin of the material dependence of superconductivity in the two families of high  $T_c$  superconductors, pnictides and cuprates. We have analyzed the superconductivity within the spin fluctuation pairing theory applied to models that take into account the realistic multi-orbital band structure. It is shown that not only in the iron pnictides, but even in the cuprates, the multi-orbital band structure is affected by the lattice structure, which in turn affects superconductivity. It is

interesting to note that in both families, the anion height measured from the cation plane plays an important role, although its effect on the band structure appears in a different manner: in the cuprates the energy difference between  $d_{x^2-y^2}$  and  $d_{z^2}$  is affected by the ligand field, while in the pnictides, the relative position between the  $d_{x^2-y^2}$  and  $d_{z^2}$  bands are affected mainly due to the variation of the band width, namely, the former (latter) band lies in the upper (lower) portion of the band structure, so that when the band width becomes wider upon lowering the height, the location of the lower band edge of  $d_{x^2-y^2}$  and that of the upper band edge of  $d_{z^2}$  (both around the wave vector  $(\pi, \pi)$ ) is exchanged. The good description of the material dependence of the superconductivity within the present approach suggests commonality between the two families in that the spin degrees of freedom are playing an important role in the occurrence of superconductivity[52], although there are differences in the strength of the electron correlation.

The present studies show that a combination of effective model construction based on first principles band calculation and application of many body theory can give a realistic description on the material dependence of superconductivity in correlated systems, and may even suggest a possibility of theoretically predicting new superconductors in the near future.

## Acknowledgment

The author would like to thank Hideo Aoki, Ryotaro Arita, and Hidetomo Usui for collaboration. The author also wishes to thank Seiichiro Onari and Katsuhiko Suzuki for collaboration in the study of pnictides, and Hirofumi Sakakibara in the study of cuprates. Numerical calculations were performed at the Information Technology Center, University of Tokyo, and at the Supercomputer Center, ISSP, University of Tokyo. This study has been supported by Grants-in-Aid for Scientific Research from MEXT of Japan and from the Japan Society for the Promotion of Science.

## References

- [1] Y. Kamihara, T. Watanabe, M. Hirano, H. Hosono: J. Am. Chem. Soc. **130** (2008) 3296.
- [2] for a review, see e.g., K. Ishida, Y. Nakai, and H. Hosono: J. Phys. Soc. Jpn. **78**, 062001 (2009).
- [3] Z.-A. Ren, W. Lu, J. Yang, W. Yi, X.-L. Shen, Z.-C. Li, G.-C. Che, X.-L. Dong, L.-L. Sun, F. Zhou, Z.-X. Zhao: Chin. Phys. Lett. **25** (2008) 2215.
- [4] L. Boeri *et al.*, Phys. Rev. Lett. **101**, 026403 (2008).
- [5] Y. Kamihara *et al.*, J. Am. Chem. Soc. **128**, 10012 (2006). *ibid* **102**, 109902(E) (2009).
- [6] C.-H. Lee *et al.* J. Phys. Soc. Jpn. **77**, 083704 (2008).
- [7] I.I. Mazin, D.J. Singh, M.D. Johannes, M.H. Du: Phys. Rev. Lett. **101** (2008) 057003.
- [8] K. Kuroki, S. Onari, R. Arita, H. Usui, Y. Tanaka, H. Kontani, and H. Aoki: Phys. Rev. Lett. **101** (2008) 087004.
- [9] J.D. Fletcher, A. Serafin, L. Malone, J. Analytis, J.-H. Chu, A.S. Erickson, I.R. Fisher, and A. Carrington, Phys. Rev. Lett. **102**, 147001 (2009).

- [10] C.W.Hicks, T.M. Lippman, M.E. Huber, J.G. Analytis, J.-H. Chu, A.S. Erickson, I.R.Fisher, and K.A.Moler, arXiv: 0903.5260.
- [11] M. Yamashita, N. Nakata, Y. Senshu, S. Tonegawa, K. Ikada, K. Hashimoto, H. Sugawara, T. Shibauchi, and Y. Matsuda : arXiv: 0906.0622.
- [12] E. Pavarini *et al.*: Phys. Rev. Lett. **87**, 047003 (2001).
- [13] K. Tanaka *et al.*: Phys. Rev. B **70**, 092503 (2004).
- [14] T. Moriya and K. Ueda: J. Phys. Soc. Jpn. **63**, 1871 (1994).
- [15] C.T. Shih *et al.*: Phys. Rev. Lett. **92**, 227002 (2004).
- [16] P. Prelovšek and A. Ramšak, Phys. Rev. B **72**, 012510 (2005).
- [17] For a review, see D.J. Scalapino : *Handbook of High Temperature Superconductivity*, Chapter 13, Eds. J.R. Schrieffer and J.S. Brooks (Springer, New York, 2007).
- [18] Th. Maier *et al.*: Phys. Rev. Lett. **85**, 1524 (2000).
- [19] P.R.C. Kent *et al.*: Phys. Rev. B **78**, 035132 (2008).
- [20] K. Kuroki, H. Usui, S. Onari, R. Arita: and H. Aoki: Phys. Rev. B **79**, 224511 (2009).
- [21] H. Sakakibara, H. Usui, K. Kuroki, R. Arita, and H. Aoki: Phys. Rev. Lett. **105**, 057003 (2010).
- [22] C.de la Cruz, Q. Huang, J. W. Lynn, Jiying Li, W. Ratcliff II, J. L. Zarestky, H. A. Mook, G. F. Chen, J. L. Luo, N. L. Wang, P. Dai: Nature **453** (2008) 899.
- [23] N. Marzari and D. Vanderbilt: Phys. Rev. B **56** (1997) 12847; I. Souza, N. Marzari and D. Vanderbilt: Phys. Rev. B **65** (2002) 035109. The Wannier functions are generated by the code developed by A. A. Mostofi, J. R. Yates, N. Marzari, I. Souza and D. Vanderbilt: (<http://www.wannier.org/>).
- [24] S. Baroni, A. Dal Corso, S. de Gironcoli, P. Giannozzi, C. Cavazzoni, G. Ballabio, S. Scandolo, G. Chiarotti, P. Focher, A. Pasquarello, K. Laasonen, A. Trave, R. Car, N. Marzari, A. Kokalj: <http://www.pwscf.org/>.
- [25] D.J. Singh and M.-H. Du: Phys. Rev. Lett. **100** (2008) 237003.
- [26] V. Vildosola, L. Pourovskii, R. Arita, S. Biermann, and A. Georges: Phys. Rev. B **78**, 064518 (2008).
- [27] S. Lebegue, Z.P. Yin, and W.E. Pickett: New J. Phys. **11**, 025004 (2009).
- [28] K. Shiraishi *et al.*: Solid State Commun. **66**, 629 (1988).
- [29] H. Kamimura and M. Eto: J. Phys. Soc. Jpn. **59**, 3053 (1990); M. Eto and H. Kamimura: J. Phys. Soc. Jpn. **60**, 2311 (1991).
- [30] A.J. Freeman and J. Yu: Physica B **150**, 50 (1988).
- [31] O.K. Andersen *et al.*: J. Phys. Chem. Solids **56**, 1573 (1995).
- [32] J.D. Jorgensen *et al.*: Phys. Rev. Lett. **58**, 1024 (1987).
- [33] J.L. Wagner *et al.*: Physica C **210**, 447 (1993).
- [34] K. Yada and H. Kontani: J. Phys. Soc. Jpn. **74** (2005) 2161.
- [35] T. Takimoto, T. Hotta, and K. Ueda: Phys. Rev. B **69** (2004) 104504.
- [36] J. Dong, H.J. Zhang, G. Xu, Z. Li, W.Z. Hu, D. Wu, G.F.Chen, X. Dai, J.L. Luo, Z.Fang, and N.L.Wang: Europhys. Lett. **83** (2008) 27006.
- [37] S. Ishibashi, K. Terakura, H. Hosono: J. Phys. Soc. Jpn. **77** (2008) 053709.
- [38] I.I. Mazin, M.D. Johannes, L. Boeri, K. Koepernik, D.J. Singh: Phys. Rev. B **78** (2008) 085104.
- [39] M.D.Lumsden, A.D.Christianson, E.A.Goremychkin, S.E. Nagler, H.A.Mook, M.B.Stone, D.L.Abemathy, T.Guidi,G.J.MacDougali, C. dela Cruz, A.S. Sefat, M.A. McGuire, B.C.Sales, and D. Mandrus: Nat. Phys. **6**, 182 (2010).
- [40] K. Kuroki and R. Arita: Phys. Rev. B **64** (2001) 024501.
- [41] K. Kuroki, T. Kimura, and R. Arita: Phys. Rev. B **66** (2002) 184508.
- [42] S.Graser, T.A. Maier, P.J. Hirshfeld, and D.J. Scalapino : New J. Phys. **11**, 025016 (2009).
- [43] A.F.Kemper, T.A.Maier, S.Graser, H.-P. Cheng, P.J. Hirshfeld, and D.J. Scalapino: arXiv:1003.2777.
- [44] H. Ikeda, R. Arita, and J. Kunes, arXiv: 1002.4471.
- [45] T. Kariyado and M. Ogata: J. Phys. Soc. Jpn. **79**, 0337803 (2010).
- [46] H. Ikeda, R. Arita, and J. Kunes: Phys. Rev. B **81**, 054502 (2010).
- [47] F. Wang, H. Zhai, D.-H. Lee: Phys. Rev. B **81**, 184512 (2010).
- [48] T. Hanaguri, S. Niitaka, K. Kuroki, and H. Takagi: Science **328**, 474 (2010).
- [49] N.E. Bickers, D.J. Scalapino, and S.R. White : Phys. Rev. Lett. **62**, 961 (1989).
- [50] T. Dahm and L. Tewordt: Phys. Rev. Lett. **74**, 793 (1995)
- [51] Y. Ohta *et al.*, Phys. Rev. B **43**, 2968 (1991).
- [52] D.J. Scalapino: axXiv:1002.2413.